UAV-Aided Two-Way Mobile Relaying Systems

Subin Eom, Hoon Lee, *Member, IEEE*, Junhee Park, and Inkyu Lee, *Fellow, IEEE*

***Abstract*— This letter investigates a two-way mobile relaying strategy where a relay mounted on a unmanned aerial vehicle (UAV) helps bidirectional communication of a pair of ground nodes (GNs). In order to deal with the minimum average rate maximization problem between two GNs, UAV trajectory, transmit power, and bandwidth are jointly optimized by fully utilizing the mobility of UAV and communication resources. To solve this problem, we apply a successive convex approximation technique for non-convex constraints by introducing new surrogate functions. Since all variables are jointly updated at the same iteration, we can yield a Karush-Kuhn-Tucker (KKT) point at the convergence point from the proposed algorithm. The effectiveness of the proposed algorithm is demonstrated in numerical results.**

***Index Terms*— UAV communication, trajectory optimization, throughput maximization, two-way relay.**

I. Introduction

As a new means for wireless communication networks, unmanned aerial vehicles (UAVs) have emerged [1]. Compared to traditional terrestrial base stations (BSs), a more flexible and cost-effective deployment is possible for UAV-mounted BSs [2]–[4]. Owing to high mobility, UAVs can effectively reduce the access distance to ground nodes (GNs) by traveling above the target area. Furthermore, UAVs tend to serve line-of-sight (LoS) channel links with GNs [5].

In order to leverage these benefits, the feasibility of UAV-aided communications has been recently studied in various scenarios. First, UAV can be used to help existing terrestrial BS-based networks for improving the quality of service (QoS) of edge users [6]. Next, as a communication relay, UAV can play an important role for GNs which do not have direct links due to obstacles, e.g., mountains and buildings. For this scenario, one-way mobile relaying protocols were introduced in [7]–[14]. In [7], trajectory of the UAV and transmit power of the UAV and GN are optimized to minimize the outage probability. The sum-power consumption of UAV and GN is minimized in [8]. The joint optimization of the transmit power and the trajectory are investigated in [9] for the rate maximization problem. Also, [10] and [11] considered a secrecy rate maximization problem for the UAV relay. In [12], sum-rate of multiple GN pairs is maximized by jointly optimizing communication resources and UAV's position. The minimum secrecy rate is maximized in [13] via jointly optimizing the UAV trajectory and time schedule. In addition, overall throughput of GNs are maximized in [14] by jointly optimizing transmit duration and power at BS and UAV relay.

For relay communications, the two-way relay protocol was designed to exchange information between GNs. The two GNs first transmit their on information to a relay at the same time. Then, the relay forwards the received data to both GNs simultaneously [15], [16]. Thus, compared to an one-way relay, the two-way relaying method is more effective as it requires only two time slots for bidirectional communications. The UAV-enabled two-way relay system was studied in [17], where the fixed UAV position and the transmission power are optimized to maximize the sum-rate.

In this letter, we propose a UAV-aided two-way mobile relaying communication system where two GNs wish to exchange information with each other through a UAV relay. A decode-and-forward (DF) strategy is adopted at the UAV relay in a frequency division duplex (FDD) mode, where the UAV decodes the uplink data collected from the GNs and transmits to the GNs through downlink which is orthogonal to the uplink channels utilized by the GNs. The transmit power, the UAV trajectory, and the bandwidth are jointly optimized in order to deal with the maximization of the minimum average rate between two GNs. Due to the difference in the one-way and the two-way relaying protocols, it is difficult to apply the solution for the one-way UAV relay network [7]–[14] to our scenario. For two-way UAV relay case [17], only UAV position is considered under the amplify-and-forward (AF) relay protocol, which cannot be applied to our scenario.

To tackle this difficulty, we utilize the successive convex approximation (SCA) technique [18]. By introducing new convex approximations for non-convex constraints, the optimization variables can be jointly updated at each iteration of SCA. Although the SCA framework has also been adopted in [9] and [10] to solve the problems, the optimality of such methods are not guaranteed in general, since they were based on alternating optimization for the trajectory and the power. In contrast, our proposed scheme achieves a Karush-Kuhn-Tucker (KKT) stationary point even though the bandwidth has been added as an additional optimization variable. By the proposed derivations, an efficient algorithm is presented, and numerical results show that the performance improvement over the baseline schemes can be achieved.

II. System Model and Problem Formulation

As presented in Fig. 1, a two-way relaying system is considered which is aided by a UAV while two GNs exchange information with each other. With the assumption that the direct link between the GNs is not available due to ground blockages, the communication between the GNs can only be

Manuscript received September 11, 2019; revised October 18, 2019; accepted November 5, 2019. Date of publication November 11, 2019; date of current version February 11, 2020. This work was supported by the National Research Foundation through the Ministry of Science, ICT, and Future Planning (MSIP), Korean Government under Grant 2017R1A2B3012316. The associate editor coordinating the review of this letter and approving it for publication was H. Tabassum. *(Corresponding author: Inkyu Lee.)*

S. Eom, J. Park, and I. Lee are with the School of Electrical Engineering, Korea University, Seoul 02841, South Korea (e-mail: esb777@korea.ac.kr; pjh0585@korea.ac.kr; inkyu@korea.ac.kr).

H. Lee is with the Department of Information and Communications Engineering, Pukyong National University, Busan 48513, South Korea (e-mail: hlee@pknu.ac.kr).

Digital Object Identifier 10.1109/LCOMM.2019.2953062

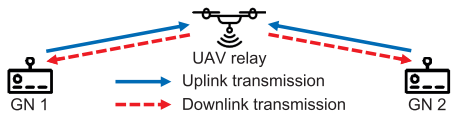

Fig. 1. Schematic diagram for UAV-aided two-way relaying systems.

achieved with the aid of the UAV relay. The locations of the GNs are assumed to be fixed, and we denote the horizontal position of GN $k \in \mathcal{K} \triangleq \{1, 2\}$ by $\mathbf{w}_k \in \mathbb{R}^{2\times 1}$.

The time period T can be discretized into N evenly divided slots, where each duration is $\delta_t = \frac{T}{N}$ [9]. Let us define the position, velocity, as well as acceleration of the UAV at time slot $n \in \mathcal{N} \triangleq \{1, \cdots, N\}$ as $\mathbf{q}[n] \in \mathbb{R}^{2\times 1}$, $\mathbf{v}[n] \in \mathbb{R}^{2\times 1}$, and $\mathbf{a}[n] \in \mathbb{R}^{2\times 1}$, respectively. Then, it follows [9]

$$\mathbf{v}[n+1] = \mathbf{v}[n] + \mathbf{a}[n]\delta_t, \quad \forall n \in \mathcal{N}, \tag{1}$$

$$\mathbf{q}[n+1] = \mathbf{q}[n] + \mathbf{v}[n]\delta_t + \frac{1}{2}\mathbf{a}[n]\delta_t^2, \quad \forall n \in \mathcal{N}. \tag{2}$$

Also, denoting $V_{\max}$ and $a_{\max}$ as the maximum speed in m/sec and the maximum acceleration in m/sec^2, respectively, the practical UAV movement constraints can be defined as

$$\|\mathbf{v}[n]\| \le V_{\max}, \ \|\mathbf{a}[n]\| \le a_{\max}, \quad \forall n \in \mathcal{N}. \tag{3}$$

Under these constraints, it is assumed that the UAV travels from a starting position $\mathbf{q}_0 \triangleq \mathbf{q}[0]$ to a final position $\mathbf{q}_F \triangleq \mathbf{q}[N]$ at a constant altitude H within T seconds.

Assuming that the Doppler effect resulted from the movement of the UAV is well handled at the GNs and the UAV, the channel gain $h_k[n]$ between GN k and the UAV at time slot n is represented as the free-space pathloss model [8]–[11]

$$h_k[n] = \frac{\gamma_0}{\|\mathbf{q}[n] - \mathbf{w}_k\|^2 + H^2}, \quad \forall k \in \mathcal{K}, \ \forall n \in \mathcal{N}, \tag{4}$$

where $\gamma_0 \triangleq \beta_0/(B\sigma^2)$ equals the signal-to-noise ratio (SNR) at 1 m as a reference. Here, β_0, B, and σ^2 indicate the channel gain at 1 m, the total bandwidth, and the power of white Gaussian noise, respectively.

Next, we explain the two-way relaying protocol for the proposed UAV communication system. The UAV employs DF relaying strategy which first decodes the data transmitted from the GNs in uplink. The decoded data is stored in a buffer at the UAV and then delivered to the GNs via the downlink channels. FDD operation is considered for uplink transmission of the GNs and downlink relaying of the UAV.

At time slot n, let us denote $\alpha_U[n] \ge 0$ and $\alpha_D[n] \ge 0$ with $\alpha_U[n] + \alpha_D[n] \le 1$ as the portion of the uplink and the downlink bandwidth allocation, respectively. Then, we have the uplink transmission rate $R_{U_k}[n]$ in bps/Hz from GN k to the UAV as

$$R_{U_k}[n] = \alpha_U[n] \log_2 \left(1 + \frac{p_{U_k}[n]h_k[n]}{p_{U_{\bar{k}}}[n]h_{\bar{k}}[n] + \alpha_U[n]}\right), \tag{5}$$

where we define $\bar{k} = 1$ for $k = 2$ and $\bar{k} = 2$ for $k = 1$, and $p_{U_k}[n]$ equals the uplink transmit power of GN k.

We assume that each GN can perform self-interference cancellation [15] to remove interference induced by its own transmit data. Thus, the downlink transmission rate $R_{D_k}[n]$ at time slot n from the UAV to GN k is denoted by [15]

$$R_{D_k}[n] = \alpha_D[n] \log_2 \left(1 + \frac{p_{D_k}[n]h_k[n]}{\alpha_D[n]}\right), \quad \forall k \in \mathcal{K}, \tag{6}$$

where $p_{D_k}[n]$ is the transmitting power from the UAV for GN k during the downlink.

In data relaying, the information causality implies that at each slot n, the relay is able to only transmit the information which has already been collected from the GNs [9]. When the processing delay at the UAV is assumed smaller than the duration of the time slot δ_t, the information causality constraint can be expressed as

$$\sum_{i=2}^{n} R_{D_k}[i] \le \sum_{i=1}^{n-1} R_{U_{\bar{k}}}[i], \quad n = 2, \ldots, N. \tag{7}$$

We consider the average and the peak power constraints both at the UAV and the GNs. Denoting $P_{U,\text{avg}}$ and $P_{D,\text{avg}}$ as the average power budgets for the GNs and the UAV, respectively, we have

$$\frac{1}{N}\sum\nolimits_{n=1}^{N-1} p_{U_k}[n] \le P_{U,\text{avg}}, \quad \forall k \in \mathcal{K}, \tag{8}$$

$$\frac{1}{N}\sum\nolimits_{n=2}^{N} \sum_{k\in\mathcal{K}} p_{D_k}[n] \le P_{D,\text{avg}}. \tag{9}$$

Also, when $P_{U,\text{peak}}$ and $P_{D,\text{peak}}$ represent the peak power constraints at the GNs and the UAV, respectively, the peak power constraints can be written by

$$0 \le p_{U_k}[n] \le P_{U,\text{peak}}, \quad \forall k \in \mathcal{K}, \ \forall n \in \mathcal{N}, \tag{10}$$

$$0 \le \sum\nolimits_{k\in\mathcal{K}} p_{D_k}[n] \le P_{D,\text{peak}}, \quad \forall n \in \mathcal{N}. \tag{11}$$

In this letter, the transmit power at the UAV and the GNs $\mathbf{P} \triangleq \{p_m[n], \ m \in \mathcal{M}, \forall n\}$, where $\mathcal{M} \triangleq \{U_1, U_2, D_1, D_2\}$, the trajectory of the UAV $\mathbf{Q} \triangleq \{\mathbf{q}[n], \mathbf{v}[n], \mathbf{a}[n], \forall n\}$, and the bandwidth allocation $\mathbf{A} \triangleq \{\alpha_U[n], \alpha_D[n], \forall n\}$ are jointly optimized to solve the minimum average rate maximization problem between the GNs. Denoting $\mathbf{O} \triangleq \{\mathbf{P}, \mathbf{Q}, \mathbf{A}\}$ as all optimization variables, the formulated problem is denoted as

$$(P1): \max_{\mathbf{O}} \min_{k\in\mathcal{K}} \frac{1}{N}\sum_{n=2}^{N} R_{D_k}[n] \tag{12a}$$

$$s.t. \quad (1)-(3), (7)-(11).$$

Because of the object and constraint in (7), (P1) is a non-convex problem. Since we consider the bandwidth allocation for the two-way relaying protocols, the existing methods in [9] and [10] for the one-way relay channels with equally allocated frequency band cannot be directly applied to our problem. Therefore, it is not straightforward to solve (P1) optimally.

III. Proposed Algorithm

In this section, we derive new convex surrogate functions for non-convex constraint and propose an efficient algorithm for solving (P1) based on the SCA technique, which iteratively solves the approximated problem of (P1). For tractable analysis, by introducing an auxiliary optimization variable $R_{\min}$ which indicates the minimum rate of the GNs, an equivalent

epigraph formulation of the minimum rate maximization problem (P1) is written as

$$(P1.1): \max_{\mathbf{O}, R_{\min}} \; R_{\min} \tag{13a}$$

$$s.t. \; \frac{1}{N}\sum_{n=2}^{N} R_{D_k}[n] \geq R_{\min}, \quad \forall k \in \mathcal{K}, \tag{13b}$$

$$(1)-(3), (7)-(11).$$

Then, we introduce a change of variable $X_{mk}[n] \triangleq p_m[n]h_k[n]$. The following lemmas present convex approximations for the new variable $X_{mk}[n]$, which are useful for determining the surrogate functions of (5) and (6).

Lemma 1: Let $x^{(l)}$ be a variable x at the l-th iteration. Then, a concave lower surrogate function $\hat{X}_{mk}^{(l)}[n]$ for $X_{mk}^{(l)}[n] \triangleq p_m^{(l)}[n]h_k^{(l)}[n]$ at a given local point $X_{mk}^{(l-1)}[n]$ can be expressed as

$$\hat{X}_{mk}^{(l)}[n] \triangleq X_{mk}^{(l-1)}[n] + (1 + X_{mk}^{(l-1)}[n])(Z_{mk}^{(l)}[n] - Y_{mk}^{(l-1)}[n]), \tag{14}$$

where

$$Y_{mk}^{(l)}[n] \triangleq \log(1 + X_{mk}^{(l)}[n]),$$

$$Z_{mk}^{(l)}[n] \triangleq \log\left(\frac{\gamma_0}{h_k^{(l-1)}[n]} + S_k^{(l)}[n] + p_m^{(l)}[n]\gamma_0\right) - \left(\log\frac{\gamma_0}{h_k^{(l-1)}[n]} + \frac{H^2 + \|\mathbf{q}^{(l)}[n] - \mathbf{w}_k\|^2 - \gamma_0/h_k^{(l-1)}[n]}{\gamma_0/h_k^{(l-1)}[n]}\right)$$

with $S_k^{(l)}[n] \triangleq 2(\mathbf{q}^{(l-1)}[n] - \mathbf{w}_k)^T(\mathbf{q}^{(l)}[n] - \mathbf{q}^{(l-1)}[n])$.

Proof: We first find upper and lower bounds for $Y_{mk}^{(l)}[n]$. Since $Y_{mk}^{(l)}[n]$ is a concave function of $X_{mk}^{(l)}[n]$, its global upper bound $Y_{mk,\text{ub}}^{(l)}[n]$ can be obtained by applying the first order Taylor approximation as

$$Y_{mk,\text{ub}}^{(l)}[n] \triangleq \log\left(1 + X_{mk}^{(l-1)}[n]\right) + \frac{X_{mk}^{(l)}[n] - X_{mk}^{(l-1)}[n]}{1 + X_{mk}^{(l-1)}[n]}.$$

Also, rewriting $Y_{mk}^{(l)}[n]$ as $Y_{mk}^{(l)}[n] = \log(\gamma_0/h_k^{(l)}[n] + p_m^{(l)}[n]\gamma_0) - \log(\gamma_0/h_k^{(l)}[n])$ and employing the first order Taylor approximation about $\mathbf{q}^{(l)}[n]$ and $p_m^{(l)}[n]$, the global lower bound $Y_{mk,\text{lb}}^{(l)}[n]$ of $Y_{mk}^{(l)}[n]$ can be calculated as $Y_{mk,\text{lb}}^{(l)}[n] \triangleq Z_{mk}^{(l)}[n]$. Since $Y_{mk,\text{ub}}^{(l)}[n] \geq Y_{mk,\text{lb}}^{(l)}[n]$ always holds, it is easy to prove $X_{mk}^{(l)}[n] \geq \hat{X}_{mk}^{(l)}[n]$, which implies that $\hat{X}_{mk}^{(l)}[n]$ is a global lower bound of $X_{mk}^{(l)}[n]$. Note that $\hat{X}_{mk}^{(l)}[n]$ is a concave function of the variables $\mathbf{q}^{(l)}[n]$ and $p_m^{(l)}[n]$. In addition, we can show that $\hat{X}_{mk}^{(l)}[n]$ satisfies other conditions of the surrogate function [18] since the first order Taylor approximated function is tight at the given local point. This completes the proof. ■

Lemma 2: A convex upper surrogate function $\check{X}_{mk}^{(l)}[n]$ for the variable $X_{mk}^{(l)}[n]$ is calculated by

$$\check{X}_{mk}^{(l)}[n] \triangleq \exp\Bigg(\log\left(\frac{\gamma_0}{h_k^{(l-1)}[n]} + p_m^{(l-1)}[n]\gamma_0\right) + \Big(H^2 + \|\mathbf{q}^{(l)}[n] - \mathbf{w}_k\|^2 - \gamma_0/h_k^{(l-1)}[n] + \gamma_0(p_m^{(l)}[n] - p_m^{(l-1)}[n])\Big)/J_{mk}^{(l-1)}[n] - \log\left(\frac{\gamma_0}{h_k^{(l-1)}[n]} + S_k^{(l)}[n]\right)\Bigg) - 1, \tag{15}$$

where $J_{mk}^{(l)}[n] \triangleq \gamma_0/h_k^{(l)}[n] + \gamma_0 p_m^{(l)}[n]$.

Proof: The proof is similar to that of Lemma 1, and thus is omitted for brevity. ■

Now, we calculate the surrogate functions of (5) and (6) based on Lemmas 1 and 2 in order to deal with non-convex constraint (7) and (13b). One can verify that a convex upper surrogate function of $c\log_2\left(1 + \frac{z}{c}\right)$ with given local point $\tilde{c}$ and $\tilde{z}$ can be computed by

$$f(c, z|\tilde{c}, \tilde{z}) \triangleq \tilde{c}\log_2\left(1 + \frac{\tilde{z}}{\tilde{c}}\right) + \left(\log_2\left(1 + \frac{\tilde{z}}{\tilde{c}}\right) - \frac{\log_2 e\ \tilde{z}}{\tilde{c} + \tilde{z}}\right)(c - \tilde{c}) + \frac{\log_2 e\ \tilde{c}}{\tilde{c} + \tilde{z}}(z - \tilde{z}). \tag{16}$$

By using (14)-(16), the surrogate functions of (5) and (6) with given local points $\alpha_U^{(l-1)}[n]$, $\alpha_D^{(l-1)}[n]$, and $X_{mk}^{(l-1)}[n]$ can be obtained as

$$R_{U_k}^{(l)}[n] \geq \hat{R}_{U_k}^{(l)}[n] \triangleq \alpha_U^{(l)}[n]\log_2\left(1 + \frac{\hat{X}_{U_k k}^{(l)}[n] + \hat{X}_{U_{\bar{k}}\bar{k}}^{(l)}[n]}{\alpha_U^{(l)}[n]}\right) - f(\alpha_U^{(l)}[n], \check{X}_{U_{\bar{k}}\bar{k}}^{(l)}[n] | \alpha_U^{(l-1)}[n], X_{U_{\bar{k}}\bar{k}}^{(l-1)}[n]), \tag{17}$$

$$R_{D_k}^{(l)}[n] \geq \hat{R}_{D_k}^{(l)}[n] \triangleq \alpha_D^{(l)}[n]\log_2\left(1 + \frac{\hat{X}_{D_k k}^{(l)}[n]}{\alpha_D^{(l)}[n]}\right), \tag{18}$$

$$R_{D_k}^{(l)}[n] \leq \alpha_D^{(l)}[n]\log_2\left(1 + \frac{\check{X}_{D_k k}^{(l)}[n]}{\alpha_D^{(l)}[n]}\right) \leq \check{R}_{D_k}^{(l)}[n] \triangleq f(\alpha_D^{(l)}[n], \check{X}_{D_k k}^{(l)}[n] | \alpha_D^{(l-1)}[n], X_{D_k k}^{(l-1)}[n]), \tag{19}$$

where $\hat{R}_{U_k}^{(l)}[n]$ and $\hat{R}_{D_k}^{(l)}[n]$ are a concave lower surrogate function of $R_{U_k}^{(l)}[n]$ and $R_{D_k}^{(l)}[n]$, respectively, and $\check{R}_{D_k}^{(l)}[n]$ denotes a convex upper surrogate function of $R_{D_k}^{(l)}[n]$. Notice that since the function $f(c, z|\tilde{c}, \tilde{z})$ is affine over c and z, we can preserve the the convexity of $\check{X}_{mk}^{(l)}[n]$.

From the above results, with the obtained solutions $\mathbf{O}^{(l-1)}$ at the $(l-1)$-th iteration, we have an approximated convex problem for (P1) at the l-th iteration as

$$(P1.2): \max_{\mathbf{O}^{(l)}, \overline{R}_{\min}} \; \overline{R}_{\min} \tag{20a}$$

$$s.t. \; \frac{1}{N}\sum_{n=2}^{N} \hat{R}_{D_k}^{(l)}[n] \geq \overline{R}_{\min}, \quad \forall k \in \mathcal{K}, \tag{20b}$$

$$\sum_{i=2}^{n} \check{R}_{D_k}^{(l)}[i] \leq \sum_{i=1}^{n-1} \hat{R}_{U_{\bar{k}}}^{(l)}[i], \quad n = 2, \ldots, N, \tag{20c}$$

$$(1)-(3), (8)-(11),$$

where $\overline{R}_{\min}$ denotes a lower bound of $R_{\min}$ in problem (P1.1). By utilizing convex optimization solvers such as CVX, we can optimally solve a convex optimization problem (P1.2).

In summary, a solution of the original problem (P1) can be obtained by iteratively solving the problem (P1.2) until convergence. For the convergence analysis of the proposed algorithm, let us define the object values of (P1.1) and (P1.2) with given local point $\mathbf{O}^{(l-1)}$ as $R_{\min}(\mathbf{O}^{(l)})$ and $\overline{R}_{\min}(\mathbf{O}^{(l)}|\mathbf{O}^{(l-1)})$, respectively. Then we can express the relationship

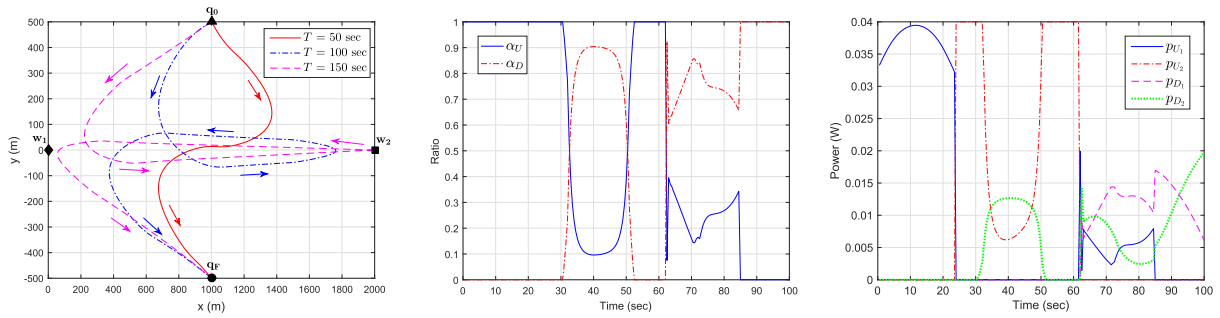

(a) UAV trajectory for various T (b) Bandwidth allocation for T = 100 sec (c) Power allocation for T = 100 sec

Fig. 2. Optimized UAV trajectory, bandwidth, and power.

$$R_{\min}(\mathbf{O}^{(l-1)}) = \overline{R}_{\min}(\mathbf{O}^{(l-1)}|\mathbf{O}^{(l-1)}) \leq \overline{R}_{\min}(\mathbf{O}^{(l)}|\mathbf{O}^{(l-1)}) \leq R_{\min}(\mathbf{O}^{(l)}), \quad (21)$$

where the first equation holds because the surrogate functions in (14)-(19) are tight at the given local points, the second inequality is derived from the non-decreasing property of the optimal solution of (P1.2), and the third inequality follows from the fact that the approximation problem (P1.2) is a lower bound of the original problem (P1.1). From (21), the objective value $R_{\min}$ in (P1.1) is non-decreasing for every iterations, and as the objective value has a finite upper bound, we can guarantee the convergence of the proposed algorithm.

Also, since the surrogate functions in (14)-(19) satisfy the conditions of the surrogate function of SCA [18] and the proposed algorithm simultaneously updates all the variables at each iteration of the SCA process, the proposed algorithm converges to at least a KKT point for (P1) [18], which means a convergence point of the proposed algorithm satisfies the necessary conditions for the globally optimal solution. This implies that the convergence point could be one of the candidates of the globally optimal solution.

The complexity analysis of the proposed algorithm can be derived as follows: Since it can be verified that (P1.2) fulfills Slater's condition, the approximated convex problem (P1.2) can be solved by applying the Lagrange duality. Then, the dual problem can be solved by using the ellipsoid method. The complexity for updating the dual variables by the ellipsoid method is $O(N^2)$ and for convergence, it takes $O(N^2)$, where N stands for the number of time slots. So, the complexity for solving (P1.2) is $O(N^4)$ [19], which accounts for the complexity of one iteration in the SCA process. Thus, denoting L as the number of iterations for convergence of the proposed algorithm, the total complexity can be expressed as $O(LN^4)$.

IV. Numerical Results

In this section, numerical results are shown in order to evaluate the proposed algorithm. For simulation settings, we fix the locations of the GNs as $\mathbf{w}_1 = [0\ 0]^T$ and $\mathbf{w}_2 = [2000\ 0]^T$ [9], and the UAV's starting position and the final destination are set to $\mathbf{q}_0 = [1000\ 500]^T$ and $\mathbf{q}_F = [1000\ \text{-}500]^T$, respectively. The power constraints are given by $P_{U,\text{avg}} = P_{D,\text{avg}} = 0.01$ W [9] and $P_{U,\text{peak}} = P_{D,\text{peak}} = 0.04$ W [3], and we consider the total bandwidth $B = 20$ MHz at the carrier frequency of 5 GHz and the reference SNR $\gamma_0 = 80$ dB [9]. The altitude of the UAV, the maximum velocity, and the maximum acceleration are determined as $H = 100$ m, $V_{\max} = 50$ m/sec [9], and $a_{\max} = 5$ m/sec^2, respectively.

We apply the trajectory initialization method in [9] and [10] where a straight line connecting the starting and ending points. Also, the bandwidth variables are initialized as $\alpha_U[n] = \alpha_D[n] = 0.5, \forall n$. To find a feasible power allocation initialization for constraint in (7), the uplink power $p_{U_k}[n]$ is set to $P_{U,\text{avg}}$, whereas the feasible downlink power is numerically found as $p_{D_k}[n] = 0.3P_{D,\text{avg}}$.

In Fig. 2(a), the optimized trajectories of the UAV for various conditions are illustrated. It can be noted in Fig. 2(a) that for all T, the UAV makes an effort to move closer to each GN to effectively help bidirectional communication of the GNs. In the case of $T = 50$ sec, the time is not long enough, so the UAV can be close to each node only one time. On the other hand, when a sufficient time is given ($T = 100, 150$ sec), an additional change in direction occurs. This result comes from the algorithm which works in a way that the data of GN 1 is first harvested and handed over to GN 2, and after that, the data of GN 2 is collected and transmitted to GN 1. In Fig. 2(b) and (c), the bandwidth and power allocation for T = 100 sec are presented, respectively. It can be seen from Fig. 2(b) that the uplink transmission from GNs is dominant for the first 30 sec to collect data from GNs. After 30 sec, the downlink transmission is carried out for relaying the information received from the GNs. Such a phenomenon can also be observed from Fig. 2(c). For the first 30 sec, the GNs transmit data to the UAV with positive power levels p_{U_1} and p_{U_2}. On the other hand, as the UAV moves toward GN 2 during 30 $\sim$ 50 sec, the UAV forwards the data to GN 2 with $\alpha_D > 0$ and $p_{D_2} > 0$. Another interesting observation is that the uplink communication is performed in an orthogonal manner to avoid multi-user interference. This can be explained through the optimized trajectory and power allocation in Fig. 2(a) and (c). We can see that the UAV first gets closer to GN 1 until 25 sec, and the channel gain between GN 1 becomes better than GN 2. Thus, GN 1 dominates the uplink transmission by utilizing p_{U_1}. After that, the data is mainly transmitted from GN 2 to the UAV as the UAV approaches GN 2. After 60 sec, the downlink transmission from the UAV is dominant to relay the received data from GNs, which can be seen in Fig. 2(b) as $\alpha_D > \alpha_U$. Unlike the uplink communication, a non-orthogonal transmission strategy

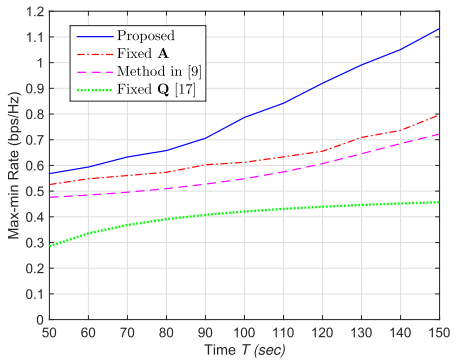

Fig. 3. Max-min rate with respect to period T.

is observed in the downlink case, i.e., p_{D_1} and p_{D_2} is generally overlapped in Fig. 2(c), thanks to self-interference cancellation at each GN.

The maximized minimum (max-min) rate of the proposed algorithm is plotted in Fig. 3 as T varies. In fact, it is not possible to directly compare the proposed algorithm with existing methods [9] and [17]. Thus, we have modified the methods in [9] and [17] to be applicable to our mobile two-way relaying systems. The following schemes are considered for the comparison.

- *Fixed* $\mathbf{A}$: The bandwidth for the uplink and the downlink is equally allocated, i.e., $\alpha_U[n] = \alpha_D[n] = 0.5,\ \forall n$. With a fixed $\mathbf{A}$, the joint optimization of the trajectory and the power is computed via the proposed algorithm.
- *Method in [9]*: A time-division modification of the one-way relaying protocol [9] is taken into account such that the UAV forwards data of GN 1 to GN 2 for the first $\frac{T}{2}$ duration, and then helps the one-way relaying from GN 2 to GN 1 in the remaining $\frac{T}{2}$ duration.
- *Fixed* $\mathbf{Q}$ *[17]*: The UAV performs relaying at the fixed position $\hat{\mathbf{q}} \triangleq \frac{\mathbf{w}_1+\mathbf{w}_2}{2}$ computed from [17]. The UAV first moves from its initial position $\mathbf{q}_0$ to the optimized location $\hat{\mathbf{q}}$. After relaying at $\hat{\mathbf{q}}$ during $\hat{T}$, the UAV moves to the final position $\mathbf{q}_F$. The time duration $\hat{T}$ during which the UAV stays at the optimized location $\hat{\mathbf{q}}$ is set to its maximum value, and the bandwidth and the power is jointly optimized at $\hat{\mathbf{q}}$ via the proposed algorithm.

From the figure, it is shown that the proposed scheme performs better than the baseline schemes for all T. Compared to the 'Fixed $\mathbf{Q}$' scheme, the proposed solution approach is crucial for the mobility-aware design aspects of the UAV networks. A performance gain of the proposed algorithm gets larger as T grows. Because the longer T, the degree of the freedom of design for the trajectory optimization becomes larger. Thus, the UAV is able to spend more time around the GNs. Also, we can see that the proposed algorithm outperforms 'Method in [9]'. Such a performance gain implies that the proposed two-way relaying protocol is important for the data exchange application. Notice that similar results have been already observed in conventional terrestrial relays which are fixed at given locations [15]. In addition, the proposed algorithm exhibits a remarkable performance gain over 'Fixed $\mathbf{A}$' scheme, meaning that the joint optimization of the bandwidth allocation is also a crucial issue for the mobile relay design.

V. Conclusion

In this letter, we have investigated the UAV-aided two-way relaying systems. The minimum rate maximization problem has been considered by addressing a joint optimization of the trajectory, the transmit power, and the bandwidth allocation. An effective SCA based algorithm which converges to a KKT point has been proposed. From the numerical results, we have demonstrated that the proposed algorithm achieves significant gains over the baseline schemes. As future works, extension to AF relay or multi-antenna at the UAV is worth pursuing. Also, multiple UAVs or GN pairs could be an important research direction.

References

[1] Y. Zeng *et al.*, "Wireless communications with unmanned aerial vehicles: Opportunities and challenges," *IEEE Commun. Mag.*, vol. 54, no. 5, pp. 36–42, May 2016.
[2] Q. Wu *et al.*, "Joint trajectory and communication design for multi-UAV enabled wireless networks," *IEEE Trans. Wireless Commun.*, vol. 17, no. 3, pp. 2109–2121, Mar. 2018.
[3] H. Lee, S. Eom, J. Park, and I. Lee, "UAV-aided secure communications with cooperative jamming," *IEEE Trans. Veh. Commun.*, vol. 67, no. 10, pp. 9385–9392, Oct. 2018.
[4] J. Park, H. Lee, S. Eom, and I. Lee, "UAV-aided wireless powered communication networks: Trajectory optimization and resource allocation for minimum throughput maximization," *IEEE Access*, vol. 7, pp. 134978–134991, Sep. 2019.
[5] S. ur Rahman *et al.*, "Positioning of UAVs for throughput maximization in software-defined disaster area UAV communication networks," *J. Commun. Netw.*, vol. 20, no. 5, pp. 452–463, Oct. 2018.
[6] N. Zhao *et al.*, "Joint trajectory and precoding optimization for UAV-assisted NOMA networks," *IEEE Trans. Commun.*, vol. 67, no. 5, pp. 3723–3735, May 2019.
[7] S. Zhang *et al.*, "Joint trajectory and power optimization for UAV relay networks," *IEEE Commun. Lett.*, vol. 22, no. 1, pp. 161–164, Jan. 2018.
[8] X. Jiang, Z. Wu, Z. Yin, and Z. Yang, "Joint power and trajectory design for UAV-relayed wireless systems," *IEEE Wireless Commun. Lett.*, vol. 8, no. 3, pp. 697–700, Jun. 2019.
[9] Y. Zeng *et al.*, "Throughput maximization for UAV-enabled mobile relaying systems," *IEEE Trans. Commun.*, vol. 64, no. 12, pp. 4983–4996, Dec. 2016.
[10] Q. Wang *et al.*, "Joint power and trajectory design for physical-layer secrecy in the UAV-aided mobile relaying system," *IEEE Access*, vol. 6, pp. 62849–62855, 2018.
[11] Q. Wang *et al.*, "Improving physical layer security using UAV-enabled mobile relaying," *IEEE Wireless Commun. Lett.*, vol. 6, no. 3, pp. 310–313, Jun. 2017.
[12] R. Fan *et al.*, "Optimal node placement and resource allocation for UAV relaying network," *IEEE Commun. Lett.*, vol. 22, no. 4, pp. 808–811, Apr. 2018.
[13] F. Cheng *et al.*, "UAV-relaying-assisted secure transmission with caching," *IEEE Trans. Commun.*, vol. 67, no. 5, pp. 3140–3153, May 2019.
[14] J. Baek *et al.*, "Optimal resource allocation for non-orthogonal transmission in UAV relay systems," *IEEE Wireless Commun. Lett.*, vol. 7, no. 3, pp. 356–359, Jun. 2018.
[15] B. Rankov and A. Wittneben, "Spectral efficient protocols for half-duplex fading relay channels," *IEEE J. Sel. Areas Commun.*, vol. 25, no. 2, pp. 379–389, Feb. 2007.
[16] K. Lee, N. Lee, and I. Lee, "Achievable degrees of freedom on MIMO two-way relay interference channels," *IEEE Trans. Wireless Commun.*, vol. 12, no. 4, pp. 1472–1480, Apr. 2013.
[17] L. Li *et al.*, "UAV positioning and power control for two-way wireless relaying," Apr. 2019, *arXiv:1904.08280*. [Online]. Available: https://arxiv.org/abs/1904.08280
[18] Y. Sun *et al.*, "Majorization-minimization algorithms in signal processing, communications, and machine learning," *IEEE Trans. Signal Process.*, vol. 65, no. 3, pp. 794–816, Feb. 2017.
[19] S. Boyd. (2017). "Ellipsoid method," Stanford University. Stanford, CA, USA. [Online]. Available: https://stanford.edu/class/ee364b/lectures/ellipsoid_method_notes.pdf